

Magnetic Quantum Wire as a Spin Filter: An Exact Study

Moumita Dey¹, Santanu K. Maiti^{1,2} and S. N. Karmakar¹

¹Theoretical Condensed Matter Physics Division,

Saha Institute of Nuclear Physics, 1/AF, Bidhannagar, Kolkata-700 064, India

²Department of Physics, Narasinha Dutt College, 129 Belilious Road, Howrah-711 101, India

We propose that a magnetic quantum wire composed of magnetic and non-magnetic atomic sites can be used as a spin filter for a wide range of applied bias voltage. We adopt a simple tight-binding Hamiltonian to describe the model where the quantum wire is attached to two semi-infinite one-dimensional non-magnetic electrodes. Based on single particle Green's function formalism all the calculations are performed numerically which describe two-terminal conductance and current through the wire. Our exact results may be helpful in fabricating mesoscopic or nano-scale spin filter.

PACS numbers: 73.63.-b, 73.63.Rt, 73.63.Nm

I. INTRODUCTION

Within the last few decades spin polarized transport phenomena [1, 2, 3] in low-dimensional systems have drawn much attention due to its potential application in the field of nanoscience and nanotechnology [4, 5]. Discovery of GMR effect [6] in Fe/Cr magnetic multilayer in 1980's has led to the development of a new branch in Condensed Matter Physics - Spintronics, which deals with the key idea of exploiting electron spin in transport phenomena. The central idea of spintronic applications involves three basic steps [7, 8], which are injection of spin through interfaces, transmission of spin through matter, and finally detection of spin. Having considerably larger spin coherence time, quantum confined nanostructures such as quantum dots and molecules are therefore ideal candidates to study spin dependent transmission which plays a significant role for further development in magnetic data storage and device processing applications and quantum computation techniques. With the increasing interest in generating pure spin current for technological purposes, modeling of spin filter is of high importance today.

Till date many theoretical [9, 10, 11, 12, 13, 14, 15, 16] and experimental efforts [17, 18] are made to design spin filter and increase the efficiency of spin polarization significantly. In 2004, Rokhinson *et al.* prepared a spin filter device using GaAs, by atomic-force microscopy with local anodic oxidation and molecular beam epitaxy methods. They were able to separate charge carriers depending on their spin state using the idea of spin-orbit interaction with a weak magnetic field. Generation of pure spin current in mesoscopic systems is a major challenge to us for further advancement in quantum computation. A more or less common trend [19, 20] to develop a spin filter theoretically is by using ferromagnetic leads or by external magnetic fields. But experimental realization of these proposals is somewhat difficult. For the first case, spin injection from ferromagnetic leads becomes difficult due to large resistivity mismatch and for the second one the difficulty is to confine a very strong magnetic field to a small region like a quantum dot (QD).

Therefore, attention is being paid for modeling of spin filter device using the intrinsic properties of quantum dots [21, 22, 23, 24, 25, 26], such as spin-orbit interaction or voltage bias. Ring shaped or Aharonov-Bohm (AB) type geometries can achieve high degree of spin polarization using Rashba spin-orbit interaction, which lifts the spin degeneracy. This has also been achieved by using an AB ring having periodic magnetic modulation.

Aim of the present paper is to study spin dependent transmission through a magnetic quantum wire which is an array of atomic sites. This system, composed of alternately placed magnetic and non-magnetic atoms, is attached symmetrically to two non-magnetic (NM) semi-infinite one-dimensional (1D) electrodes. A simple tight-binding Hamiltonian is used to describe the system where all the calculations are done by using single particle Green's function formalism [27, 28, 29, 30, 31, 32, 33]. With the help of Landauer formula spin dependent conductance is obtained, and the current-voltage characteristics are computed from the Landauer-Büttiker formalism [34, 35, 36]. We explore various features of spin transport using this simple geometry. Quite interestingly, we see that for a certain energy range, transmission probability of up spin electron drops to zero, whereas for down spin electrons it becomes non-zero and vice-versa. Therefore, tuning the Fermi energy (E_F) of the system, the magnetic quantum wire can be used as a spin filter for a wide range of applied bias voltage depending on the strength of localized magnetic moments in the wire.

The scheme of the paper is as follow. With a brief introduction (Section I), in Section II, we describe the model and theoretical formulations for the calculation. Section III explores the significant results which explain the filtering action, and finally, we conclude our study in Section IV.

II. MODEL AND SYNOPSIS OF THE THEORETICAL BACKGROUND

The schematic representation of our model is depicted in Fig. 1. In this figure we illustrate the nano-structure

through which spin dependent transport is investigated. We study spin transmission through a quantum wire of N atomic sites composed of alternately placed magnetic and non-magnetic atoms. The wire is attached symmetrically to two non-magnetic semi-infinite 1D metallic electrodes termed as source and drain. The atomic sites forming the device are of 3 different types. One of them being non-magnetic and the other two being magnetic of types A and B, having two different values of localized magnetic moments, h_A and h_B , associated with them. The orientation of the local moments associated with each magnetic site is specified by angles θ_n and ϕ_n (n denotes the n -th site) in spherical polar coordinate system. The

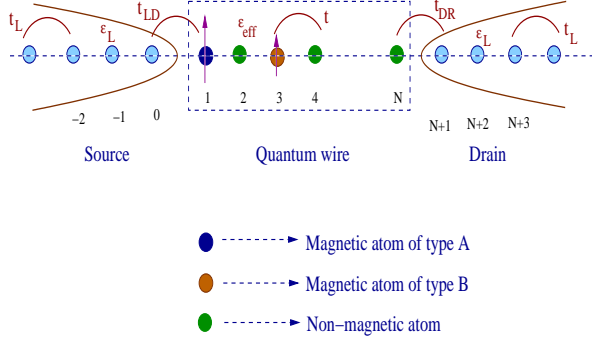


FIG. 1: (Color online). A magnetic quantum wire (framed region) of N atomic sites attached to two semi-infinite 1D NM electrodes, namely, source and drain. Filled green circles correspond to NM atomic sites, while the filled blue and brown circles represent atomic sites having unequal magnetic moments.

two metallic electrodes consist of infinite number of non-magnetic atoms labeled as $0, -1, -2, \dots, -\infty$ for the left electrode and $(N+1), (N+2), (N+3), \dots, \infty$ for the right one.

For the whole system (source-wire-drain) we can write the Hamiltonian as,

$$H = H_W + H_L + H_R + H_{LW} + H_{WR} \quad (1)$$

where, H_W corresponds to the Hamiltonian of the wire. $H_{L(R)}$ represents the Hamiltonian for the left (right) electrode, and $H_{LW(WR)}$ is the Hamiltonian representing the wire-electrode coupling.

The spin polarized Hamiltonian for the quantum wire can be written in effective one-electron approximation, within the tight-binding formalism in Wannier basis, using nearest-neighbor approximation as,

$$H_W = \sum_{n=1}^N \mathbf{c}_n^\dagger \left(\epsilon_0 - \mathbf{h}_n \cdot \vec{\sigma} \right) \mathbf{c}_n + \sum_{i=1}^N \left(\mathbf{c}_i^\dagger \mathbf{t} \mathbf{c}_{i+1} + \text{h.c.} \right) \quad (2)$$

where,

$$\mathbf{c}_n^\dagger = \begin{pmatrix} c_{n\uparrow}^\dagger & c_{n\downarrow}^\dagger \end{pmatrix} \\ \mathbf{c}_n = \begin{pmatrix} c_{n\uparrow} \\ c_{n\downarrow} \end{pmatrix} \\ \epsilon_0 = \begin{pmatrix} \epsilon_0 & 0 \\ 0 & \epsilon_0 \end{pmatrix} \\ \mathbf{t} = t \begin{pmatrix} 1 & 0 \\ 0 & 1 \end{pmatrix} \\ \mathbf{h}_n \cdot \vec{\sigma} = h_n \begin{pmatrix} \cos \theta_n & \sin \theta_n e^{-i\phi_n} \\ \sin \theta_n e^{i\phi_n} & -\cos \theta_n \end{pmatrix}$$

First term of Eq. (2) represents the effective on-site energies of the atomic sites in the wire. ϵ_0 's are the site energies, while the $\mathbf{h}_n \cdot \vec{\sigma}$ refers to the interaction of the spin (σ) of the injected electron with the localized on site magnetic moments. This term is responsible for spin flipping at the sites. Second term describes the nearest-neighbor hopping strength between the sites of the quantum wire.

Similarly, the Hamiltonian $H_{L(R)}$ can be written as,

$$H_{L(R)} = \sum_i \mathbf{c}_i^\dagger \epsilon_{L(R)} \mathbf{c}_i + \sum_i \left(\mathbf{c}_i^\dagger \mathbf{t}_{L(R)} \mathbf{c}_{i+1} + \text{h.c.} \right) \quad (3)$$

where, $\epsilon_{L(R)}$'s are the site energies of the electrodes and $t_{L(R)}$ is the hopping strength between the nearest-neighbor sites of the left (right) electrode.

Here also,

$$\epsilon_{L(R)} = \begin{pmatrix} \epsilon_{L(R)} & 0 \\ 0 & \epsilon_{L(R)} \end{pmatrix} \\ \mathbf{t}_{L(R)} = \begin{pmatrix} t_{L(R)} & 0 \\ 0 & t_{L(R)} \end{pmatrix}$$

The wire-electrode coupling Hamiltonian is described by,

$$H_{LW(WR)} = \left(\mathbf{c}_{0(N)}^\dagger \mathbf{t}_{LW(WR)} \mathbf{c}_{1(N+1)} + \text{h.c.} \right) \quad (4)$$

where, $t_{LW(WR)}$ being the wire-electrode coupling strength.

In order to calculate the spin dependent transmission probabilities and the current through the magnetic quantum wire we use single particle Green's function technique. Within the regime of coherent transport and for non-interacting systems this formalism is well applied.

The single particle Green's function representing the full system for an electron with spin σ is defined as [27, 28, 29],

$$\mathbf{G}_\sigma = (\mathbf{E} - \mathbf{H}_\sigma)^{-1} \quad (5)$$

where,

$$\mathbf{E} = (\epsilon + i\eta)\mathbf{I} \quad (6)$$

ϵ being the energy of the electron passing through the system. $i\eta$ is a small imaginary term added to make the Green's function (G_σ) non-hermitian.

Now \mathbf{H}_σ and \mathbf{G}_σ representing the Hamiltonian and the Green's function for the full system can be partitioned like [27, 28, 29],

$$\mathbf{H}_\sigma = \begin{pmatrix} \mathbf{H}_{L\sigma} & \mathbf{H}_{LW\sigma} & 0 \\ \mathbf{H}_{LW\sigma}^\dagger & \mathbf{H}_{W\sigma} & \mathbf{H}_{WR\sigma} \\ 0 & \mathbf{H}_{WR\sigma}^\dagger & \mathbf{H}_{R\sigma} \end{pmatrix} \quad (7)$$

$$\mathbf{G}_\sigma = \begin{pmatrix} \mathbf{G}_{L\sigma} & \mathbf{G}_{LW\sigma} & 0 \\ \mathbf{G}_{LW\sigma}^\dagger & \mathbf{G}_{W\sigma} & \mathbf{G}_{WR\sigma} \\ 0 & \mathbf{G}_{WR\sigma}^\dagger & \mathbf{G}_{R\sigma} \end{pmatrix} \quad (8)$$

where, $\mathbf{H}_{L\sigma}$, $\mathbf{H}_{R\sigma}$, and $\mathbf{H}_{W\sigma}$ represent the Hamiltonians (in matrix form) for the left electrode (source), quantum wire and right electrode (drain), respectively. $\mathbf{H}_{LW\sigma}$ and $\mathbf{H}_{WR\sigma}$ are the matrices for the Hamiltonians representing the wire-electrode coupling strength. Assuming that there is no coupling between the electrodes themselves, the corner elements of the matrices are zero. Similar definition goes for the Green's function matrix G_σ as well.

Our first goal is to determine $\mathbf{G}_{W\sigma}$ (Green's function for the wire only) which defines all physical quantities of interest. Following Eq. (5) and using the block matrix form of \mathbf{H}_σ and \mathbf{G}_σ the form of $\mathbf{G}_{W\sigma}$ can be expressed as [27, 28, 29],

$$\mathbf{G}_{W\sigma} = (\mathbf{E} - \mathbf{H}_{W\sigma} - \boldsymbol{\Sigma}_{L\sigma} - \boldsymbol{\Sigma}_{R\sigma})^{-1} \quad (9)$$

where, $\boldsymbol{\Sigma}_{L\sigma}$ and $\boldsymbol{\Sigma}_{R\sigma}$ represent the contact self-energies introduced to incorporate the effects of semi-infinite electrodes coupled to the system, and, they are expressed by the relations [27, 28, 29],

$$\boldsymbol{\Sigma}_{L\sigma} = \mathbf{H}_{LW\sigma}^\dagger \mathbf{G}_{L\sigma} \mathbf{H}_{LW\sigma} \quad (10)$$

$$\boldsymbol{\Sigma}_{R\sigma} = \mathbf{H}_{WR\sigma}^\dagger \mathbf{G}_{R\sigma} \mathbf{H}_{WR\sigma}$$

Thus the form of self-energies are independent of the nano-structure itself through which transmission is studied and they completely describe the influence of electrodes attached to the system. Now, the transmission probability (T_σ) of an electron with spin σ is related to the Green's function as [27, 28, 29],

$$T_\sigma = \text{Tr}[\boldsymbol{\Gamma}_{L\sigma} \mathbf{G}_{W\sigma}^r \boldsymbol{\Gamma}_{R\sigma} \mathbf{G}_{W\sigma}^a] \quad (11)$$

where, $\mathbf{G}_{W\sigma}^r$ and $\mathbf{G}_{W\sigma}^a$ are the retarded and advanced single particle Green's functions (for the device only) for an electron with spin σ . $\boldsymbol{\Gamma}_{L\sigma}$ and $\boldsymbol{\Gamma}_{R\sigma}$ are the coupling matrices, representing the coupling of the magnetic quantum wire to the left and right electrodes, respectively, and they are defined by the relation [27, 28, 29],

$$\boldsymbol{\Gamma}_{L\sigma(\mathbf{R}\sigma)} = \mathbf{i}[\boldsymbol{\Sigma}_{L\sigma(\mathbf{R}\sigma)}^r - \boldsymbol{\Sigma}_{L\sigma(\mathbf{R}\sigma)}^a] \quad (12)$$

Here, $\boldsymbol{\Sigma}_{L\sigma(\mathbf{R}\sigma)}^r$ and $\boldsymbol{\Sigma}_{L\sigma(\mathbf{R}\sigma)}^a$ are the retarded and advanced self-energies, respectively, and they are conjugate to each other. It is shown in literature by Datta *et al.*

that the self-energy can be expressed as a linear combination of a real and imaginary parts in the form,

$$\boldsymbol{\Sigma}_{L\sigma(\mathbf{R}\sigma)}^r = \boldsymbol{\Lambda}_{L\sigma(\mathbf{R}\sigma)} - \mathbf{i}\boldsymbol{\Delta}_{L\sigma(\mathbf{R}\sigma)} \quad (13)$$

The real part of self-energy describes the shift of the energy levels and the imaginary part corresponds to broadening of the levels. The finite imaginary part appears due to incorporation of the semi-infinite electrodes having continuous energy spectrum. Therefore, the coupling matrices can be easily obtained from the self-energy expression and is expressed as,

$$\boldsymbol{\Gamma}_{L\sigma(\mathbf{R}\sigma)} = -2\text{Im}(\boldsymbol{\Sigma}_{L\sigma(\mathbf{R}\sigma)}) \quad (14)$$

Considering linear transport regime, conductance (g_σ) is obtained using Landauer formula [27, 28, 29],

$$g_\sigma = \frac{e^2}{h} T_\sigma \quad (15)$$

Knowing the transmission probability (T) of an electron with spin σ , the current (I_σ) through the system is obtained using Landauer-Büttiker formalism. It is written in the form [27, 28, 29],

$$I_\sigma(V) = \frac{e}{h} \int_{-\infty}^{+\infty} [f_L(E) - f_R(E)] T_\sigma(E) dE \quad (16)$$

where, $f_{L(R)} = f(E - \mu_{L(R)})$ gives the Fermi distribution function of the two electrodes having chemical potentials $\mu_{L(R)} = E_F \pm eV/2$. E_F is the equilibrium Fermi energy.

III. NUMERICAL RESULTS AND DISCUSSION

All the essential features of spin transport through a magnetic quantum wire are studied by performing several numerical calculations. Here, we assume that the non-magnetic 1D metallic electrodes are made from identical materials, therefore, the site energies and the nearest-neighbor hopping strengths are chosen to be identical for the two electrodes. Let us begin our discussion by mentioning the values of different parameters used for numerical calculations. We choose the quantum wire to be made up of 64 ($N = 64$) sites. The on-site energies (ϵ_0) in the quantum wire are chosen to be 0. Magnitudes of the two different local magnetic moments h_A and h_B associated with two types of magnetic sites A and B are set as 1.9 and 0.1. The hopping strength between the nearest-neighbor sites of the magnetic quantum wire and for the two NM electrodes are set at $t = 3$ and $t_L = t_R = 4$, respectively. The site energies ($\epsilon_{L(R)}$) of all the sites in the two electrodes are fixed at 0. For the sake of simplicity, we choose the unit where $h = c = e = 1$. Throughout the analysis we study the basic features of spin transport for two distinct regimes of electrode-to-magnetic quantum wire coupling.

Case 1: Weak-coupling limit.

This regime is defined by the criterion $t_{LW(WR)} \ll t$. In this case, we choose the values as $t_{LW} = t_{WR} = 0.5$.

Case 2: Strong-coupling limit.

This limit is described by the condition $t_{LW(WR)} \sim t$. In this regime we choose the values of hopping strengths as $t_{LW} = t_{WR} = 2.5$.

A. Conductance-energy spectrum

To explain all the relevant features of spin transport we start with the conductance-energy characteristics. As illustrative examples, first in Fig. 2 we plot the variation of conductance g with respect to the energy E for up (\uparrow) and down (\downarrow) spin electrons separately in the limit of weak

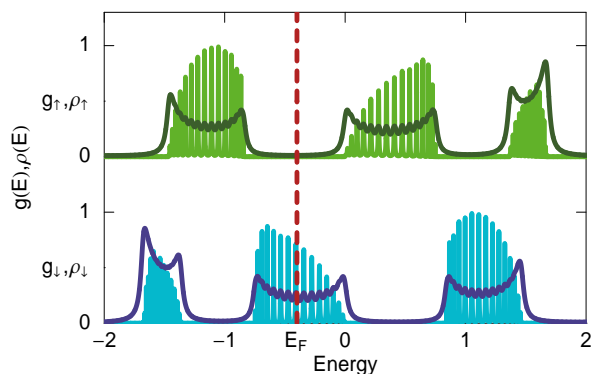


FIG. 2: (Color online). g - E and ρ - E (thick solid lines) curves in the limit of weak-coupling for a magnetic quantum wire with $N = 64$. Upper and lower panels correspond to the results of up and down spin electrons, respectively. Dotted line represents the location of Fermi energy E_F of the wire.

wire-electrode coupling strength. Also, the variation of average density of states (ADOS) are superimposed in each case. The mathematical description for the ADOS (symbolized as $\rho(E)$) of the magnetic quantum wire including the effect of the two electrodes for an electron with spin σ is expressed as,

$$\rho_\sigma(E) = -\frac{1}{N\pi} \text{Im} [\text{Tr}[\mathbf{G}\mathbf{w}_\sigma]] \quad (17)$$

It is observed from the conductance spectra that up and down spin electrons follow entirely two different channels while passing through the wire. This splitting of up and down conduction channels is responsible for *spin filtering* action. Quite interestingly we see that for a certain range of energy for which the transmission probability (T_\uparrow) and hence the conductance (g_\uparrow) for up spin electron drops to zero value, shows non-zero transmission probability (T_\downarrow) as well as conductance (g_\downarrow) due to down spin electron. The presence of sharp resonant peaks in the conductance spectrum are associated with the energy eigenvalues of the full system. In this case due to large system size,

$N = 64$, the sharp resonant peaks get closely spaced to form a quasi band as shown by the green and blue regions.

In the limit of strong wire-electrode coupling as shown in Fig. 3, transmission probability (T_σ) almost reaches to the value unity and the sharp conductance peaks acquire some broadening which is quantified by the imaginary part of the self-energy expression, incorporated to include the effect of semi-infinite electrodes. The feature of broadening is not very clear from this figure due to large system size. Apart from increase in transmission probability and broadening of conductance peaks, all the other

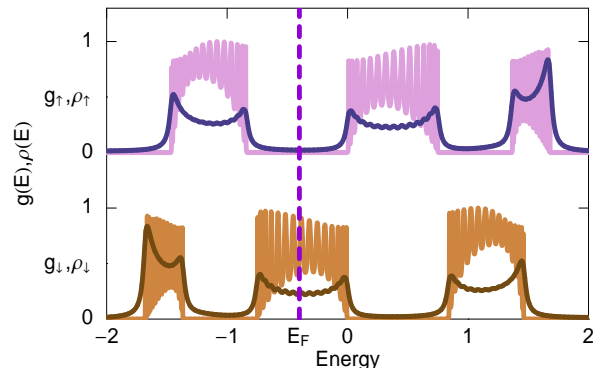


FIG. 3: (Color online). g - E and ρ - E (thick solid lines) curves in the limit of strong-coupling for a magnetic quantum wire with $N = 64$. Upper and lower panels correspond to the results of up and down spin electrons, respectively. Dotted line represents the location of Fermi energy E_F of the conductor.

features, as observed in the weak-coupling case, remain the same e.g., formation of quasi bands and position of band gaps. Therefore, increase in electrode-wire coupling strength does not change the position of global gaps in the conductance spectrum, but the coupling has a strong influence in the study of current-voltage characteristics as discussed clearly in the references [30, 31, 32, 33].

B. Degree of polarization vs. energy spectrum

Next, in Fig. 4 we show the variation of degree of polarization (DOP) with respect to the energy of the injected electrons. For a particular energy value E , the DOP is defined in terms of transmission probabilities T_σ in the following way,

$$\text{DOP}(E) = \left| \frac{T_\uparrow(E) - T_\downarrow(E)}{T_\uparrow(E) + T_\downarrow(E)} \right| \quad (18)$$

DOP gives a quantitative measurement of the spin polarization achieved. It is observed from Fig. 4 that the degree of polarization is significantly enhanced with the increase in wire-to-electrode coupling strength and for wide range of energies it (DOP) almost reaches to the value unity or 100% as expressed conventionally in most of the literatures. Thus our proposed model quantum

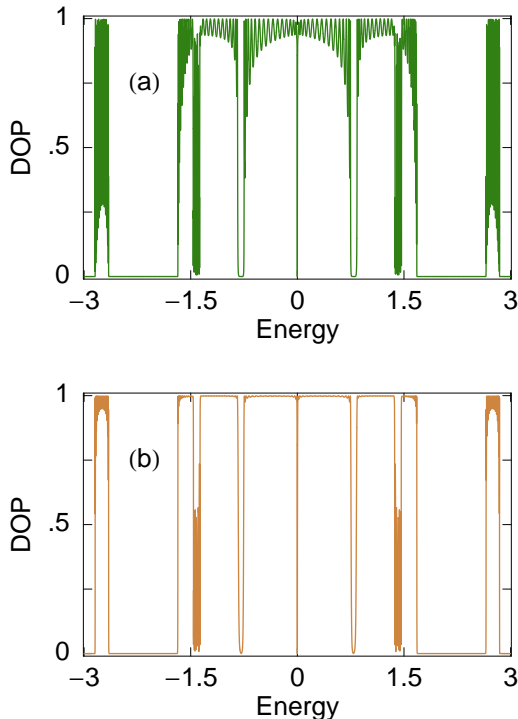


FIG. 4: (Color online). Degree of polarization as a function of energy for a magnetic quantum wire with $N = 64$. (a) weak-coupling limit and (b) strong-coupling limit.

system is a very good example for designing a *spin filter*.

C. Current-voltage characteristics

The spin filtering action becomes clearer in the current-voltage (I - V) characteristics presented in Fig. 5. Current across the magnetic quantum wire is obtained by integrating over the transmission function following Landauer-Büttiker formalism for a constant Fermi energy (E_F). In this case we set the value of E_F at -0.4 (dotted line in Fig. 3). As this value of E_F falls in the energy gap region of the up spin conductance spectrum, therefore, non-zero value of up spin current is obtained after overcoming a finite value of the applied bias voltage, the so-called threshold voltage (V_{th}). On the other hand, for any given bias voltage V , non-zero value of down spin current is observed. Thus spin filtering takes place up to the bias voltage (V_{th}), when up spin current is totally blocked and only down spin current is obtained. In an exactly similar way, if we set the Fermi energy at some value of down spin energy gap region, down spin current can be blocked totally by passing the up spin current only. Here, we plot the current-voltage characteristics only in the strong-coupling limit. Exactly a similar filtering action is also observed in the case of weak-coupling limit. But the point is that in the limit of strong-coupling, current amplitude gets magnified significantly compared to

the weak-coupling limit. The plateau like structures in the current-voltage characteristics are observed due to the presence of global gaps in the conductance spectrum.

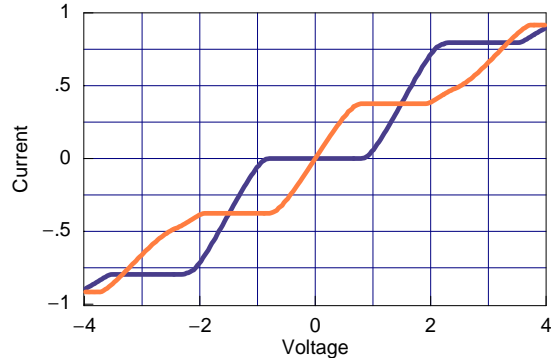


FIG. 5: (Color online). Current I as a function of bias voltage V in the limit of strong-coupling for a magnetic quantum wire with $N = 64$. The blue and orange curves correspond to the currents for up and down spin electrons, respectively.

The value of V_{th} depends on the difference between the localized magnetic moments associated with the magnetic atoms. Therefore, changing the atoms the magnitude of V_{th} can be tuned.

IV. CONCLUDING REMARKS

To conclude, in the present paper we have investigated spin transport through a magnetic quantum wire using single particle Green's function formalism. We have adopted a simple tight-binding framework to illustrate the system, which is a quantum wire formed by magnetic and non-magnetic atomic sites and connected symmetrically to source and drain. We have shown the variation of conductance as a function of injecting electron energy for up and down spin electrons separately for two different strengths of wire-to-electrode coupling. Conductance spectrum clearly depicts the splitting of up and down spin conduction channels which is the key idea behind the modeling of a spin filter. Larger the difference between the local magnetic moments of the two types of magnetic atoms, smaller is the overlap between the up and down conduction channels. Also we have plotted the variation of degree of polarization with respect to energy for both the coupling regimes. It shows that enhancement of coupling strength increases the degree of polarization i.e., improves the quality of filtration significantly. Finally, we have obtained the current passing through the device using Landauer-Büttiker formulation. The feature of spin filtering is visualized more prominently in the current-voltage characteristics. Tuning the Fermi energy to a particular value the device can act as a spin filter i.e., up to a certain range of bias voltage only up or down spin current is obtained.

In this work we have calculated all these results by ignoring the effects of temperature, spin-orbit interac-

tion, electron-electron correlation, electron-phonon interaction, disorder, etc. Here, we fix the temperature at 0K, but the basic features will not change significantly even in non-zero finite (low) temperature region as long as thermal energy ($k_B T$) is less than the average energy spacing

of the energy levels of the magnetic quantum wire. In this model it is also assumed that the two side-attached non-magnetic electrodes have negligible resistance.

All these predicted results using such a simple geometry may be useful in designing a spin polarized source.

-
- [1] S. A. Wolf *et al.*, Science **294**, 1488 (2001).
 [2] G. Prinz, Science **282**, 1660 (1998).
 [3] G. Prinz, Phys. Today **48**, 58 (1995).
 [4] J. Chen, M. A. Reed, A. M. Rawlett, and J. M. Tour, Science **286**, 1550 (1999).
 [5] P. Ball, Nature (London) **404**, 918 (2000).
 [6] M.N.Baibich, J. M. Broto, A. Fert, F. N. Van Dau, F. Petroff, P. Etienne, G. Creuzet, A. Friederich, and J. Chazelas, Phys. Rev. Lett. **61**, (1998) 2472.
 [7] J. Stöhr and H. C. Siegmann, *Magnetism- From Fundamental to Nanoscale Dynamics*, Springer (2006).
 [8] S. Maekawa and T. Shinjo, *Spin Dependent Transport in Magnetic Nanostructures*, CRC Press (2002).
 [9] H. Yin, T. Lü, X. Liu, and H. Xue, Phys. Lett. A **285**, 373 (2009).
 [10] F. Chi and S. Li, J. Appl. Phys. **100**, 113703 (2006).
 [11] M. W. Wu, J. Zhou, and Q. W. Shi, Appl. Phys. Lett. **6**, 85 (2004).
 [12] A. A. Shokri, M. Mardaani, and K. Esfarjani, Physica E, **27**, 325 (2005).
 [13] F. Chi, X. Yuan, and J. Zheng, Nanoscale Res. Lett. **3**, 343 (2008).
 [14] M. Lee and C. Bruder, Phys. Rev. B **73**, 085315 (2006).
 [15] J. H. Ojeda, M. Pacheco, and P. A. Orellana, Nanotechnology **20**, 434013 (2009).
 [16] K. Chang and F. M. Peeters, Solid State Commun. **120**, 181 (2001).
 [17] Rokhinson *et al.* Phys. Rev. Lett. **93**, 146601 (2004).
 [18] D. Jin, Z. Li, M. Xiao, G. Jin, and A. Hu, J. Appl. Phys. **99**, 08T304 (2004).
 [19] W. Long, Q. F. Sun, H. Guo, and J. Wang, Appl. Phys. Lett. **83**, 1397 (2003).
 [20] P. Zhang, Q. K. Xue, and X. C. Xie, Phys. Rev. Lett. **91**, 196602 (2003).
 [21] Q. F. Sun and X. C. Xie, Phys. Rev. B **91**, 235301 (2006).
 [22] Q. F. Sun and X. C. Xie, Phys. Rev. B **71**, 155321 (2005).
 [23] F. Chi, J. Zheng, and L. L. Sun, Appl. Phys. Lett. **92**, 172104 (2008).
 [24] T. P. Pareek, Phys. Rev. Lett. **92**, 076601 (2004).
 [25] W. J. Gong, Y. S. Zheng, and T. Q. Lü, Appl. Phys. Lett. **92**, 042104 (2008).
 [26] H. F. Lü and Y. Guo, Appl. Phys. Lett. **91**, 092128 (2007).
 [27] S. Datta, *Electronic transport in mesoscopic systems*, Cambridge University Press, Cambridge (1997).
 [28] S. Datta, *Quantum Transport: Atom to Transistor*, Cambridge University Press, Cambridge (2005).
 [29] D. A. Ryndyk, R. Gutiérrez, B. Song, and G. Cuniberti, arXiv:0805.0628v2.
 [30] S. K. Maiti, J. Phys. Soc. Jpn. **78**, 114602 (2009).
 [31] S. K. Maiti, Phys. Lett. A **373**, 4470 (2009).
 [32] S. K. Maiti, Solid State Commun. **149**, 1684 (2009).
 [33] S. K. Maiti, Solid State Commun. **149**, 1623 (2009).
 [34] R. Landauer, Phys. Lett. A **85**, 91 (1986).
 [35] R. Landauer, IBM J. Res. Dev. **32**, 306 (1988).
 [36] M. Büttiker, IBM J. Res. Dev. **32**, 317 (1988).